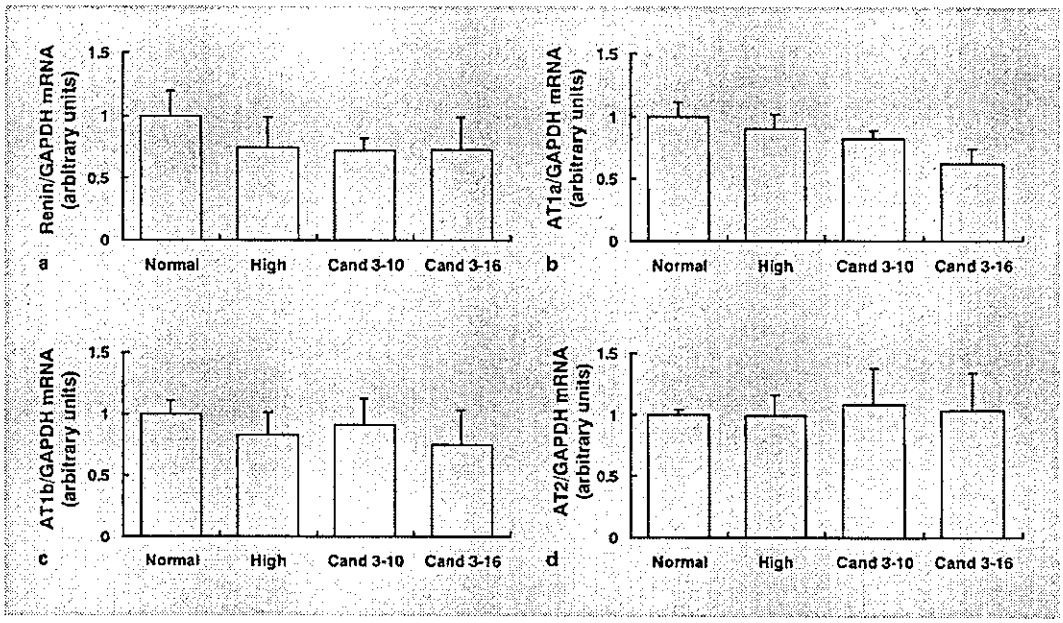

Fig. 6. Quantitation of signals from RT-PCR of renin/GAPDH and AT receptor/GAPDH mRNA in the kidneys of 16-week-old Dahl-S rats. Normal: group 1 (normal salt diet); High: group 2 (high salt diet); Cand 3–10: group 3 (high salt diet + candesartan cilexetil (3–10 weeks)); Cand 3–16: group 4 (high salt diet + candesartan cilexetil (3–16 weeks)).

hypertension, and in the effects of these agents in preventing end-organ damage [10]. This led us to hypothesize that this particular model would be the most difficult to treat using our prepubertal approach.

As noted in the introduction, previous studies by our and other groups have shown that early treatment with ACEI or ARB attenuates the development of hypertension, as well as the development of hypertensive nephrosclerosis in SHR and its derivative strain (SHRSP) [2–5]. Moreover the effect was associated with a permanent attenuation in the renin-angiotensin system [5]. Since overactivation of the renin-angiotensin system has been shown to be involved in the pathophysiology of both the hypertension and end-organ damage in these rats [11, 12], these results suggested that suppression of the renin-angiotensin system could be involved in the mechanism of the protection afforded by prepubertal treatment with ARB. In this study, we asked what would be the effect in the Dahl-S rat, which already has a suppressed renin-angiotensin system.

We found that the prepubertal treatment with ARB resulted in a reduction in blood pressure, which continued for 6 weeks after discontinuation of the drug. The blood pressure in the rats treated prepubertally with ARB remained at a value of approximately 150 mm Hg, whereas the blood pressure in the untreated rats was greater than 200 mm Hg. Although the rats treated continuously with ARB had a blood pressure reduction which was significantly greater at 15 weeks and 16 weeks, the blood pressure difference between groups 3 and 4 during these last 2 weeks was small, and substantially less than the marked reduction of greater than 50 mm Hg compared to group 2. Of note, the magnitude of this reduction was similar to that seen in our previous study using SHRSP rats [5]. It would have been interesting to see if the blood pressure remained decreased at time points later than 16 weeks. However, the Dahl-S rat has a short lifespan, with a dramatic increase in stroke-related deaths from as early as 11–13 weeks [13, 14], resulting in less than 40% survival at 19 weeks. Indeed, we found signs suggestive of stroke at 16 weeks in three rats, which led us to conclude the study at this age.

We next examined cardiovascular hypertrophy in the treated and untreated rats. We found that a significant difference in the heart weight/body weight ratios could not be detected between the treated and untreated rats on

a high salt diet. In the case of aortic wall thickness, a statistically significant reduction was detectable in rats treated continuously with ARB, but the suppression of vascular hypertrophy was incomplete. These results are interesting because, as noted above, the blood pressures in the treated groups were well controlled to approximately 140–150 mm Hg. One possible explanation for these findings could be that the cardiovascular hypertrophy induced by a high-salt diet in Dahl-S rats may be caused in part by a blood pressure-independent mechanism [15].

We next examined if the prepubertal treatment had a lasting renoprotective effect. Compared to the untreated rats on a high salt diet, the rats treated prepubertally with ARB had a statistically significant decrease in proteinuria, suggesting a renoprotective effect. To confirm these findings, renal tissue was examined microscopically, and it was found that the results of histological scoring were similar to the results for proteinuria, Of interest, we found that values of plasma total cholesterol showed exactly the same trend as the changes in proteinuria. Because the elevated cholesterol in Dahl-S rats has been attributed to be secondary to proteinuria [16], it is probable that the reduction in total cholesterol is an added benefit secondary to the renoprotective effect.

One possible interpretation of our findings is that the short treatment with ARB from 3–10 weeks may have merely delayed the onset of nephropathy (by 7 weeks). In this case, we would expect a rightward shift of 7 weeks in the time course of development of proteinuria. The fact that we did not find such a rightward shift makes this possibility less likely, and suggest that other mechanisms may be involved in the renoprotective effect.

In our previous study, we found that prepubertal treatment with angiotensin inhibitors caused a sustained decrease in plasma levels of renin and angiotensin II, as well as a decrease in kidney renin mRNA [5]. In this study, we found that the renin levels in the control rats were low, and that the values remained suppressed after salt-loading and ARB treatment. Plasma angiotensin II levels were below the detection limit in all the groups. Similarly, no significant differences in renal renin mRNA were detectable between the groups. We also examined AT receptor subtype mRNA levels, because we have previously found that ARB treatment can cause changes in renal AT receptor subtype mRNA expression [8], however no significant changes were detectable in this model.

What then are the potential mechanisms for the sustained reduction in blood pressure seen in the rats treated temporarily with ARB? One possibility is the suppression of a vascular amplifier mechanism, which has been suggested by some groups to be involved in the development of hypertension [17]. According to this hypothesis, increased blood pressure may lead to vascular hypertrophy and structural changes which initiates a positive feedback loop leading to further blood pressure elevation. Blockade of angiotensin II actions may inhibit the vascular amplifier mechanism by attenuating the rise in blood pressure or by inhibiting the vascular trophic actions of this peptide or both. Because we did not find marked changes in the cardiovascular hypertrophy in this study, the role of inhibition of vascular amplifier mechanism in the observed changes remains uncertain. Another possibility is that changes in central nervous system control of blood pressure may have occurred in the treated rats. Of interest, Wu et al. reported that early treatment of SHR with captopril impairs central responses to angiotensin I and II, suggesting that treatment of rats at a young age with renin-angiotensin system inhibitors may lead to permanent changes in central nervous system function [3]. A third possibility is that hormones other than renin and angiotensin (for example arginine vasopressin) may have been altered by the early treatment protocol [18]. These possibilities are not mutually exclusive, and it is possible that multiple mechanisms may be involved in the sustained suppression of blood pressure seen in this study.

The results of this study have several important implications for the design of a strategy to limit and possibly to 'cure' hypertension and hypertensive renal damage. Such a strategy could be of great clinical importance for renal diseases other than hypertensive nephrosclerosis, since many renal diseases, including polycystic kidney disease, which is the most common autosomal dominant genetic disorder, have a strong genetic component. At present, there appears to be no effective way to attenuate the propensity to renal disease in such patients.

Firstly, our results support the hypothesis that prepubertal treatment with angiotensin inhibitors affords sustained, albeit partial protection from renal injury, even in a animal model with a suppressed renin-angiotensin system. Although the effects of prepubertal intervention have not been studied in other models, it is interesting that Moulder et al. have reported that treatment with ACEI or ARB during a time window of 4–10 weeks after radiation injury can attenuate radiation-induced nephropathy in rats [19]. Further studies are required to examine if the results of this study are applicable to other models of renal disease, and if a similar therapeutic approach would be effective or practical in humans with severe genetic renal diseases.

Secondly, we found several similarities as well as differences with the SHR model. The blood pressure was reduced by approximately 50 mm Hg in both cases, yet the prepubertal treatment was not very effective in suppressing cardiovascular hypertrophy in either model [5]. In the case of the kidney, a clear renoprotective effect was found in both models, however the protection was partial and not complete in the case of the Dahl-S rat, whereas almost complete protection was seen with the SHRSP. We speculate that the differences with the results for SHRSP arise from the fact that the prepubertal treatment caused a significant suppression in the renin-angiotensin system in the case of SHRSP, whereas no such change was detectable in the Dahl rats. These results are compatible with the assumption that activation of the renin-angiotensin system may worsen renal damage independently of blood pressure in SHRSP [11, 12]. In the case of the Dahl-S rats, blood pressure reduction alone in the absence of major alterations in the renin-angiotensin system may have resulted in the partial renoprotection afforded by the short-treatment protocol.

Thirdly, our results suggest the need for renoprotective therapy which is tailor-made to the underlying pathophysiology. Since treatment with ARB alone does not provide complete renoprotection in this model, the addition of a different agent may be required. For example, it has been proposed that activation of the endothelin system may be involved in the pathophysiology of renal damage in the Dahl-S rat [20, 21]. If this is the case, further studies are required to see if combined prepubertal treatment with other inhibitors (for example an endothelin receptor antagonist) may provide a more complete renoprotective effect.

In conclusion, the results of this study indicate that prepubertal treatment with ARB results in a prolonged reduction in blood pressure and partial renoprotection even in an animal model with a suppressed renin-angiotensin system. We speculate that prepubertal intervention may indeed be an effective strategy for preventing renal disease in later life, however combination treatment with different agents may be required, depending on the underlying pathophysiology of the renal disease.

References

1 Kaplan N, Lieberman E: Clinical Hypertension, ed 7. Philadelphia, Lippincott, Williams and Wilkins, 1998.
2 Harrap SB, Van der Merwe WM, Griffin SA, Macpherson F, Lever AF: Brief angiotensin converting enzyme inhibitor treatment in young spontaneously hypertensive rats reduces blood pressure long-term. Hypertension 1990; 16:603–614.
3 Wu JN, Berecek KH: Prevention of genetic hypertension by early treatment of spontaneously hypertensive rats with the angiotensin converting enzyme inhibitor captopril. Hypertension 1993;22:139–146.
4 Traub O, Lloyd MC, Webb RC: Long-term effects of brief antihypertensive treatment on systolic blood pressure and vascular reactivity in young genetically hypertensive rats. Cardiovasc Drugs Ther 1995;9:421–429.
5 Nakaya H, Sasamura H, Hayashi M, Saruta T: Temporary treatment of prepubescent rats with angiotensin inhibitors suppresses the development of hypertensive nephrosclerosis. J Am Soc Nephrol 2001;12:659–666.
6 Katovich MJ, Gelband CH, Reaves P, Wang HW, Raizada MK: Reversal of hypertension by angiotensin II type 1 receptor antisense gene therapy in the adult SHR. Am J Physiol 1999; 277:H1260–264.
7 Mackenzie HS, Troy JL, Rennke HG, Brenner BM: TCV 116 prevents progressive renal injury in rats with extensive renal mass ablation. J Hypertens Suppl 1994;12:S11–16.
8 Nakaya H, Sasamura H, Kitamura Y, Amemiya T, Konishi K, Hayashi M, Saruta T: Effects of angiotensin inhibitors on renal injury and angiotensin receptor expression in early hypertensive nephrosclerosis. Hypertens Res 1999; 22:303–312.
9 Rapp JP, Dene H: Development and characteristics of inbred strains of Dahl salt-sensitive and salt-resistant rats. Hypertension 1985;7: 340–349.
10 Leenen FH, Yuan B: Prevention of hypertension by irbesartan in Dahl S rats relates to central angiotensin II type 1 receptor blockade. Hypertension 2001;37:981–984.
11 Shibota M, Nagaoka A, Shino A, Fujita T: Renin-angiotensin system in stroke-prone spontaneously hypertensive rats. Am J Physiol 1979;236:H409–416.
12 Volpe M, Camargo MJ, Mueller FB, Campbell WG, Jr, Sealey JE, Pecker MS, Sosa RE, Laragh JH: Relation of plasma renin to end organ damage and to protection of K+ feeding in stroke-prone hypertensive rats. Hypertension 1990;15:318–326.
13 Zhang JJ, Chao L, Chao J: Adenovirus-mediated kallikrein gene delivery reduces aortic thickening and stroke-induced death rate in Dahl salt-sensitive rats. Stroke 1999;30:1925–1931;discussion 1931–1932.
14 Kodama K, Adachi H, Sonoda J: Beneficial effects of long-term enalapril treatment and low-salt intake on survival rate of dahl salt-sensitive rats with established hypertension. J Pharmacol Exp Ther 1997;283:625–629.
15 Zhao X, White R, Van Huysse J, Leenen FH: Cardiac hypertrophy and cardiac renin-angiotensin system in Dahl rats on high salt intake. J Hypertens 2000;18:1319–1326.
16 Yoneda H, Toriumi W, Ohmachi Y, Okumura F, Fujimura H, Nishiyama S: Involvement of angiotensin II in development of spontaneous nephrosis in Dahl salt-sensitive rats. Eur J Pharmacol 1998;362:213–219.
17 Folkow B: The debate on the amplifier hypothesis – some comments. J Hypertens 2000;18: 375–378.
18 Zhang L, Edwards DG, Berecek KH: Effects of early captopril treatment and its removal on plasma angiotensin converting enzyme (ACE) activity and arginine vasopressin in hypertensive rats (SHR) and normotensive rats (WKY). Clin Exp Hypertens 1996;18:201–226.
19 Moulder JE, Fish BL, Cohen EP: Brief pharmacological intervention in experimental radiation nephropathy. Radiat Res 1998;150:535–541.
20 Ikeda T, Ohta H, Okada M, Kawai N, Nakao R, Siegl PK, Kobayashi T, Maeda S, Miyauchi T, Nishikibe M: Pathophysiological roles of endothelin-1 in Dahl salt-sensitive hypertension. Hypertension 1999;34:514–519.
21 Barton M, Vos I, Shaw S, Boer P, D'Uscio LV, Grone HJ, Rabelink TJ, Lattmann T, Moreau P, Luscher TF: Dysfunctional renal nitric oxide synthase as a determinant of salt-sensitive hypertension: mechanisms of renal artery endothelial dysfunction and role of endothelin for vascular hypertrophy and glomerulosclerosis. J Am Soc Nephrol 2000;11:835–845.

Histochem Cell Biol (2003) 119:257–264
DOI 10.1007/s00418-003-0511-x

ORIGINAL PAPER

Teiko Ohashi · Keiko Uchida · Shinichi Uchida ·
Sei Sasaki · Hiroshi Nihei

Intracellular mislocalization of mutant podocin and correction by chemical chaperones

Accepted: 18 February 2003 / Published online: 8 March 2003

Abstract The NPHS2 gene encoding the podocin protein was causally linked to the autosomal recessive type of steroid-resistant nephrotic syndrome. In this study, we investigated the consequence of the R138Q mutation of podocin, one of the most common missense mutations in the NPHS2 gene, by examining the expression of the wild-type and R138Q mutant podocins in mammalian cells. Either myc- or FLAG-tagged wild-type podocin was strongly stained in plasma membrane, particularly in the fine processes wherein the protein was colocalized with actin stress fibers. On the other hand, the R138Q mutant podocin was completely retained intracellularly and colocalized with the endoplasmic reticulum (ER) marker, calnexin. These results suggest that the R138Q mutation affected podocin protein folding, thereby interfering with the mutant protein's departure from the ER. To determine if the ER retention of R138Q mutant is correctable, cells were incubated with the chemical chaperones glycerol, trimethylamine-N-oxide, and DMSO. Using these two methods, namely, cell surface labeling with sulfo-NHS-S-S-biotin and Alexa 488-streptavidin, and immunostaining to detect the podocin protein close to the plasma membrane, we confirmed that these chemical chaperone treatments elicit a cellular redistribution of R138Q podocin. Our results reveal defective cellular processing of the mutant podocin, and provide evidence for pharmacological correction of the processing defect.

T. Ohashi · K. Uchida (✉) · H. Nihei
Department of Medicine, Kidney Center,
Tokyo Women's Medical University,
8-1 Kawada-cho Shinjuku, 162-8666 Tokyo, Japan
e-mail: kuchida@kc.twmu.ac.jp
Tel.: +81-3-33538111 Ext. 39112
Fax: +81-3-33560293

S. Uchida · S. Sasaki
Homeostasis Medicine and Nephrology,
Graduate School, School of Medicine,
Tokyo Medical and Dental University,
1-5-45 Yushima Bunkyo, 113-8519 Tokyo, Japan

Keywords Podocyte · Cell surface expression · Nephrosis · Immunohistochemistry · ER retention

Introduction

Podocin is a podocyte-specific stomatin-like protein (Boute et al. 2000) produced by NPHS2, the gene responsible for the autosomal recessive type of steroid-resistant nephrotic syndrome (SRNS). Several nonsense and missense mutations of NPHS2 have been identified in patients with non-familial focal segmental glomerulosclerosis as well as patients with autosomal recessive SRNS (Boute et al. 2000; Caridi et al. 2001; Frishberg et al. 2002; Karle et al. 2002). At the time of this writing, however, the pathological consequences of these podocin mutations have not been investigated. According to a report by Boute et al. (2000), the R138Q mutation was most commonly found in patients with autosomal recessive SRNS.

In this study, we isolated the human podocin cDNA by reverse transcription PCR and built expression constructs possessing the amino terminal FLAG epitope or carboxy terminal myc epitope. Using these constructs, we transiently expressed the wild-type and mutant podocins in opossum kidney (OK) cells and SV-40-transformed human podocytes (Tsutsui et al. 1997), and then determined whether the mutation affected cellular localization of the podocin. We found that the wild-type podocin was localized in the plasma membrane whereas the R138Q mutation resulted in the accumulation within the endoplasmic reticulum (ER). Several mutant membrane proteins such as CFTR (Denning et al. 1992; Welsh and Smith 1993) and the AQP2 water channel have also been shown to remain in the ER (Tamarappoo and Verkman 1998; Tamarappoo et al. 1999; Hirano et al. 2002), and chemical chaperone treatment in vitro has been shown to correct this ER retention (Tamarappoo and Verkman 1998; Tamarappoo et al. 1999). In this study, we investigated whether chemical chaperones were effective in releasing the R138Q mutant retained in the ER to the plasma membrane.

Materials and methods

Construction of cDNAs encoding the wild-type and R138Q mutant podocins

Human podocin cDNA was obtained by reverse transcription PCR using human kidney mRNA as a template with the following primers: 5'-CCGAATTCAGCCGCCCGGCAGCTCTGAGGATG and 5'-CCGGATCCTAACATGGGAGAGTCTTTCTTTTTAGGATT. The PCR product of the expected size was cut with EcoRI and BamHI at the sites incorporated into the ends of the primers and cloned into pCDNA3.1(−) myc-His A vector (Invitrogen, Carlsbad, Calif., USA) and p3xFLAG-mycCMV-26 vector (Sigma, St. Louis, Mo., USA). Constructs were confirmed by sequencing. A point mutation at R138 was generated by the Quick Change site-directed mutagenesis kit (Strategene, La Jolla, Calif., USA).

Cell culture and transient transfection

The OK cells and SV-40-transformed human podocytes (Tsutsui et al. 1997) were grown in DMEM and RPMI-1640 with 10% fetal calf serum, respectively. For immunofluorescence studies, the wild-type and mutant cDNAs in the expression plasmids were transfected into cells grown on type I collagen-coated cover glasses with Lipofectamin 2000. Immunofluorescence detection was performed 24 h after transfection. Chemical chaperone treatment [1 M glycerol, 100 mM trimethylamine oxide (TMAO), or 2% DMSO] was commenced 20 h after the transfection.

Immunofluorescence and confocal laser scanning microscopy

Transfected cells were fixed in PBS containing 2% paraformaldehyde, permeabilized with 0.1% Triton X-100 if necessary, and then blocked for 1 h at 37°C in 1% BSA/PBS. Podocin was immunostained using anti-myc antibody (9E10) (Santa Cruz Biotechnology, Santa Cruz, Calif., USA) or anti-FLAG M2 antibody (Sigma), and then observed by LSM510 confocal microscopy. Actin stress fibers (AFs) were visualized by Alexa 488-conjugated phalloidin (Molecular Probes, Eugene, Ore., USA) binding. Antibodies to GM130 and calnexin were obtained from BD Biosciences (San Jose, Calif., USA) and Santa Cruz Biotechnology, respectively.

Cell surface biotinylation

Cells were washed three times with ice-cold PBS with 0.1 mM $CaCl_2$ and 1 mM $MgCl_2$ (PBS-CM), then incubated for 15 min with 1.0 mg/dl EZ-link sulfo-NHS-S-S-biotin (Pierce, Rockford, Ill., USA) in a cold biotinylation buffer (150 mM NaCl, 2 mM $CaCl_2$, 10 mM triethanolamine, pH 9.0). After washing with quenching buffer (192 M glycine, 25 mM TRIS, in PBS-CM), cell surface biotin was visualized by Alexa 488-conjugated streptavidin.

Western blotting

One day after transfection, the cells were harvested using RIPA buffer and proteins were resolved in SDS-PAGE. Myc-tagged and FLAG-tagged podocins were detected by 9E10 anti-myc and M2 anti-FLAG monoclonal antibodies, respectively. Phosphorylated ERK was detected by anti-pErk antibody (Promega, Madison Wis., USA). Bands were detected by alkaline phosphatase-conjugated secondary antibody and western blue (Promega).

Results

Transient expression of wild-type and R138Q podocins in OK cells and human podocytes

As shown in Fig. 1, the wild-type and R138Q podocin proteins were both detected in OK cells and podocytes using anti-myc antibody in western analyses. FLAG-tagged podocins were also detected by M2 antibody or anti-FLAG polyclonal antibody (Sigma; data not shown). Figure 2 shows immunofluorescence of the wild-type and R138Q podocins in OK cells (Fig. 2a) and podocytes (Fig. 2b). As shown in the *left panels*, the wild-type podocin was stained in plasma membrane, particularly in the fine processes wherein the wild-type podocin appeared to be closely localized with the AFs (Fig. 2a *lower panel*). In contrast, the R138Q mutant podocin was retained intracellularly in both cell lines.

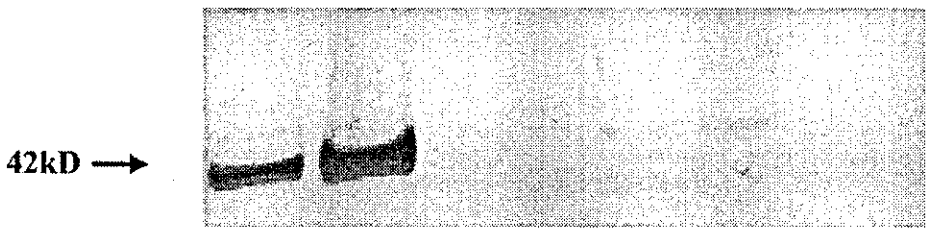

Fig. 1 Western blot of the wild-type and R138Q podocin expressed transiently in opossum kidney (*OK*) cells and human SV-40-transformed podocytes. Expression vectors were transfected into OK cells and podocytes using Lipofectamine 2000 (Invitrogen) according to the manufacturer's recommendation. Twenty-four hours after transfection, cells were harvested with RIPA buffer and resolved in SDS-PAGE. To detect myc-tagged podocin, a monoclonal 1:200 dilution of anti-myc antibody (9E10) was used as a primary antibody, and then the signal was detected by alkaline phosphatase-conjugated anti-mouse IgG antibody and western blue (Promega). A 42-kDa band (*arrow*) and the upper bands were detected in cells transfected with a vector plus podocin inserts, but not in cells transfected with a vector only

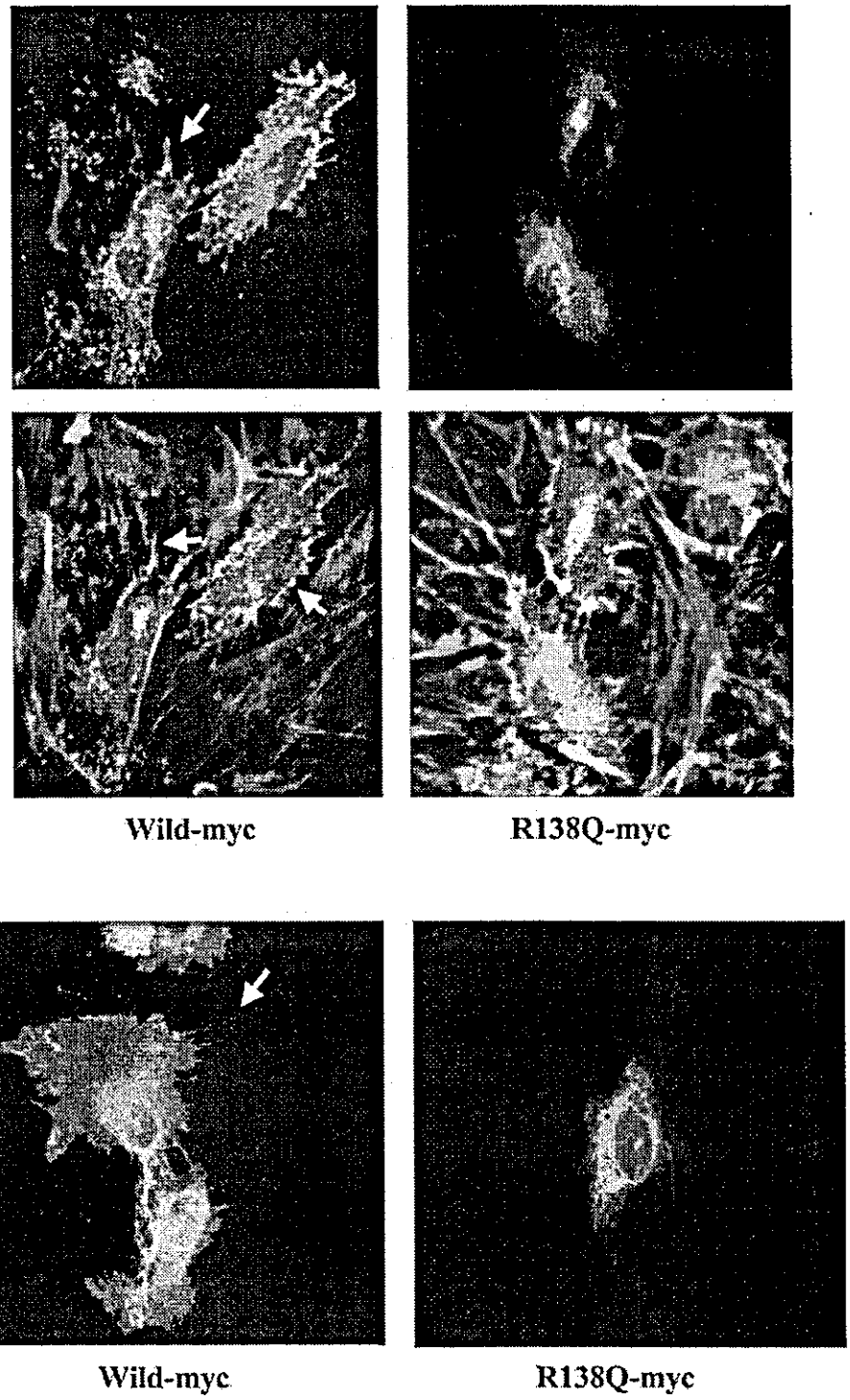

Fig. 2a, b Immunohistochemistry of myc-tagged wild-type and R138Q podocins in OK cells (**a**) and podocytes (**b**). Myc-tagged podocins were detected with anti-myc antibody (9E10) and Alexa 546 (*red*)-conjugated anti-mouse IgG, and actin stress fibers (AFs) were visualized by Alexa 488-conjugated phalloidin binding (*green*) in the *lower panel* of **a**, in which *arrows* indicate the close localization of the wild-type podocin and AFs. ×630

Intracellular localization of R138Q

To determine where the R138Q was retained within the cells, double immunofluorescence was performed for podocin with several known intracellular organelle markers. As shown in Fig. 3a, b, the R138Q was best colocalized with calnexin, an ER membrane protein, while GM130, a Golgi marker, was partially colocalized with R138Q. From these data, R138Q was identified to be retained mainly in the ER.

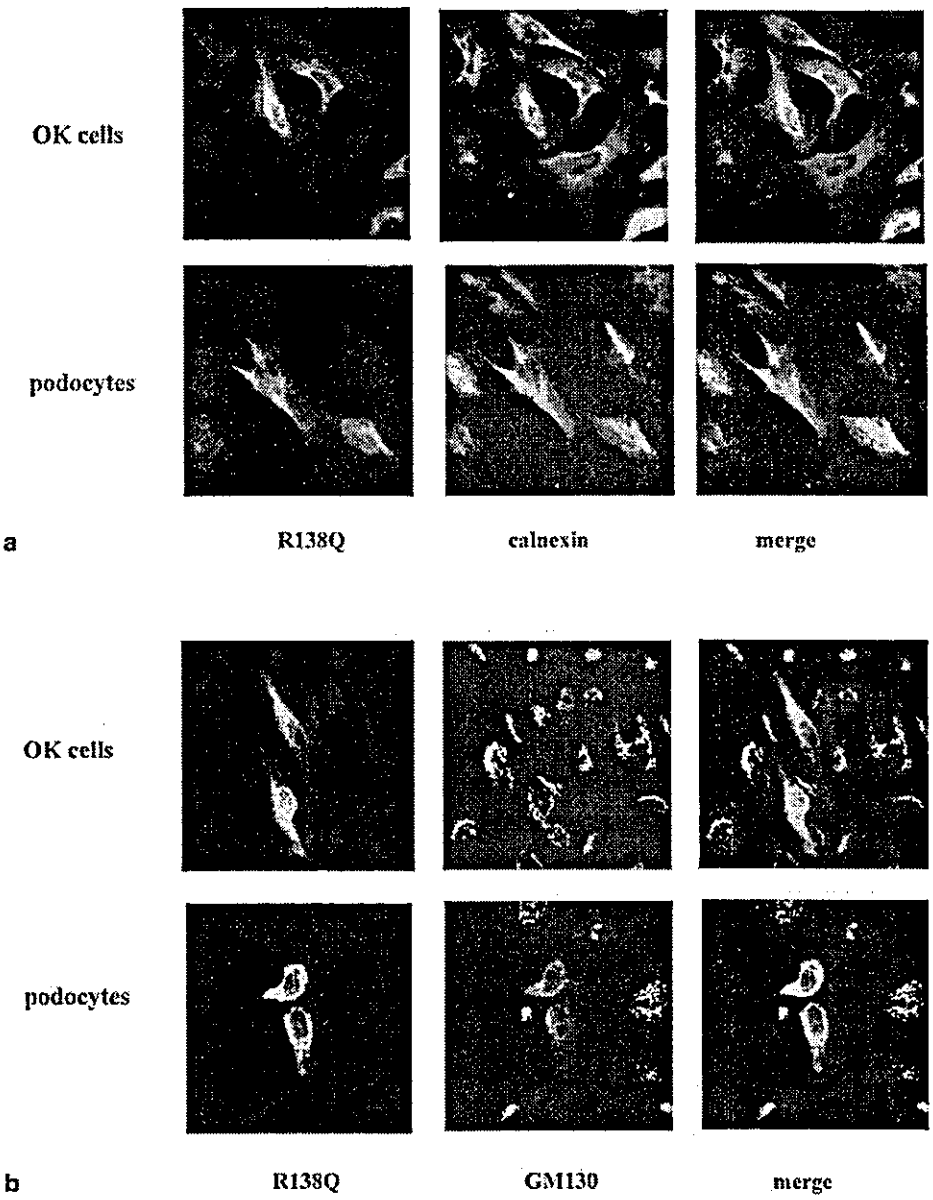

Fig. 3a, b Double immunolabeling of R138Q podocin and calnexin (a) or GM130 (b). R138Q was detected by Alexa 546 (*red*). Calnexin and GM130 were detected by Alexa 488 (*green*). ×400

Chemical chaperone treatment of the R138Q podocin

Next, we tried to determine whether chemical chaperones might be effective in correcting ER localization of the R138Q podocin. In previous reports on mutant CFTR and the AQP2 water channel (Welsh and Smith 1993; Tamarappoo and Verkman 1998; Tamarappoo et al. 1999), some ER-retained mutants were released to plasma membrane by chemical chaperone treatment. As shown in Fig. 4, OK cells transfected with the R138Q-myc were incubated with either 1 M glycerol, 100 mM TMAO, or 2% DMSO. Unlike the case with the podocin staining without these treatments, the staining (red) in TMAO- and DMSO-treated cells appeared to spread toward plasma membrane labeled by biotin (green). To further confirm the plasma membrane localization of the released R138Q podocin, we took advantage of the characteristics of the amino terminally FLAG-tagged podocin in immunofluorescence. It has been shown that stomatin, a podocin-related protein, has a hairpin-like structure wherein both amino and carboxy termini are present intracellularly (Salzer et al. 1993; Huang et al. 1995). At the time of this writing, it remains unknown whether podocin shares a similar structure. As shown in Fig. 5a, Triton X treatment was necessary for the detection of carboxy terminally myc-tagged podocin, but not for the detection of the amino terminally FLAG-tagged wild-type podocin. We are not certain that the amino terminus resides outside the cell surface since the fixation with 2% paraformaldehyde might have partially permeabilized the cells. Our result

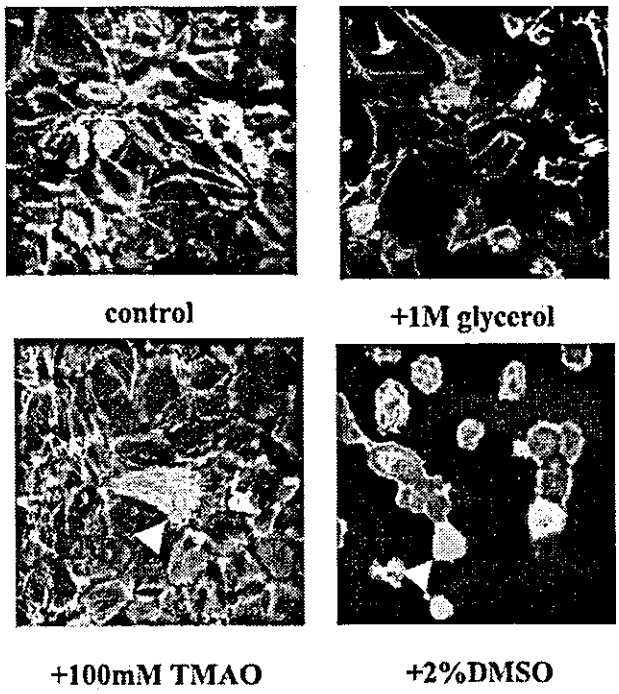

Fig. 4 Effect of chemical chaperones on the intracellular localization of the R138Q podocin in OK cells. OK cells transiently expressing the R138Q podocin were treated with 1 M glycerol, 100 mM trimethylamine oxide (TMAO), or 2% DMSO for 4 h. Twenty-four hours after transfection, cells were treated with sulfo-NHS-S-S-biotin and fixed. Cell surface biotin was detected by Alexa 488-conjugated streptavidin (*green*). R138Q was stained (*red*) by the method described previously. As shown by the *arrowheads*, the intracellularly retained R138Q shown in the control panel appeared to be released to the plasma membrane in the presence of 100 mM TMAO and 2% DMSO; 1 M glycerol appeared to have less effect. x400

suggests, however, that if the amino terminus resides within the cells, it does so in very close proximity to the plasma membrane. We took advantage of this feature and determined the cellular localization of FLAG-tagged R138Q podocin. As shown in the lower panels in Fig. 5a, the FLAG-R138Q staining was found intracellularly and was dependent upon Triton X treatment. In contrast, Fig. 5b, c shows that the FLAG-R138Q in cells with chemical chaperone treatment appeared to be stained along the plasma membrane even without Triton X treatment. This clearly further supports that the chemical treatment was effective in releasing the ER-retained R138Q podocin.

ERK activation by wild-type and R138Q podocin expression

Recently, Huber et al. (2001) reported that the coexpression of podocin and nephrin induced AP-1 activity via activation of p38 kinase and JNK. We tested whether the similar phenomenon was observed in our cells and whether the R138Q mutation affected the ability to induce the signaling. As shown in Fig. 6, no podocin-induced phosphorylation of ERK1 or 2 was detected in OK cells. In contrast, the wild-type podocin and the R138Q, each induced ERK2 phosphorylation in podocytes. The lack of ERK2 activation in OK cells might be due to the lack of endogenous nephrin expression.

Discussion

Since the initial identification of the NEPH2 gene encoding podocin as a key molecule for the glomerular filtration barrier, several mutations of the NEPH2 gene have been reported in familial and non-familial cases of SRNS (Boute et al. 2000; Caridi et al. 2001; Frishberg et al. 2002; Karle et al. 2002; Tsukaguchi et al. 2002; Winn 2002). However, no one has yet clarified how these mutations influence biological function at a cellular level. More recently, podocin was found to bind CD2AP and nephrin at its carboxy terminus (Huber et al. 2001; Schwarz et al. 2001). On the basis of this finding, we can speculate that the binding of podocin to nephrin may be impaired by nonsense mutations that lead to the truncation of the carboxy terminus or insertion/deletion type mutations that induce frameshifts of the carboxy terminal portion of podocin, thereby eliciting the loss of function of these protein complexes. In contrast, the pathological basis of the missense mutations of podocin remains entirely unknown. Since the R138Q mutation is one of the most common mutations in the NPHS2 gene (Boute et al. 2000; Caridi et al. 2001), we focused on this mutant in this study. The first objective of this study was to determine the cellular localizations of the wild-type and R138Q podocins in mammalian cells. The second objective was to determine whether the trafficking of the mutant podocin was a primary defect, and if it was, to develop a pharmacological strategy to correct this nephrosis-linked defect.

As shown in Figs. 1 and 2, we detected the expressions of wild-type podocin and R138Q podocin by western blotting and immunohistochemistry in SV-40-transformed podocytes and OK cells. In immunohistochemistry, the wild-type podocin exhibited a cell surface distribution, especially in the fine processes. This staining pattern was quite similar to the immunohistochemistry of endogenous podocin in cultured podocytes recently reported by Saleem et al. (2002). Though not completely colocalized within cells, the wild-type podocin was localized in close proximity to the AFs, especially in the fine processes (see the *arrows* in the *left lower panel* of Fig. 2a). Saleem et al. (2002) reported a similar finding in cultured podocytes, i.e., colocalization of nephrin and podocin with actin cytoskeleton at the tip of the AFs. They also found that the disruption of actin filaments abolished the cell surface localizations of nephrin and podocin. These results confirmed that our transient expression system reflected the cellular localization of endogenously expressed podocin. In the course of these experiments, we also

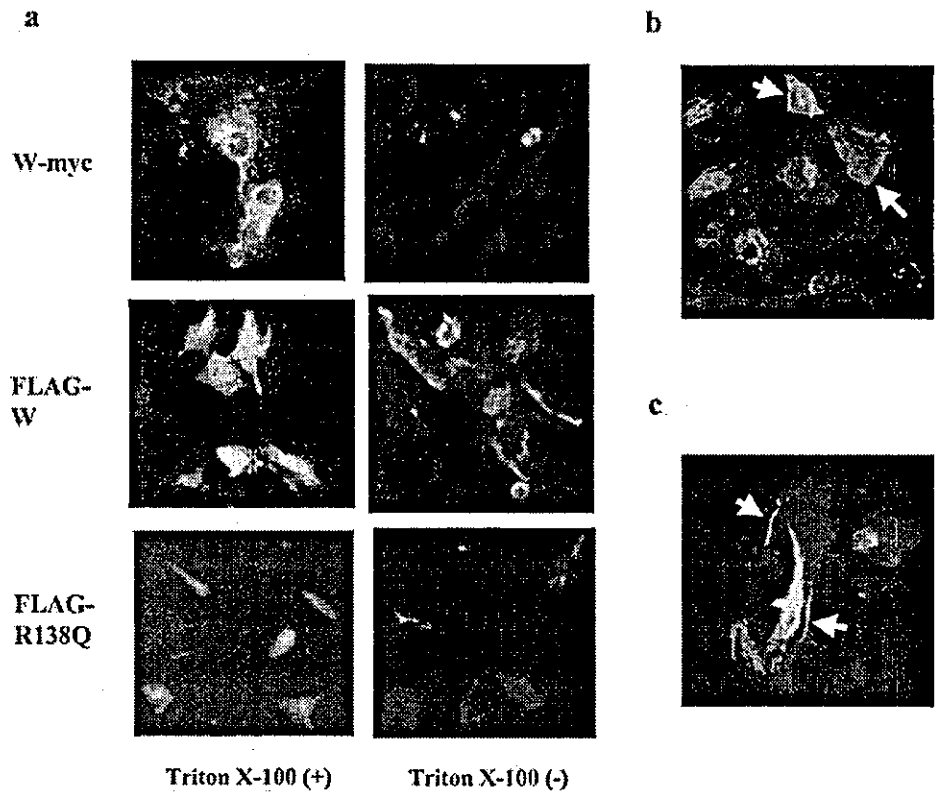

Fig. 5a–c Detection of podocins with FLAG epitope at the amino terminus and the release of R138Q to the plasma membrane in the presence of chemical chaperones. **a** *Upper panels* Wild-type podocin tagged with myc epitope at its carboxy terminus was only detected with permeabilization using 0.1% Triton X after fixation. ×400. *Middle panels* Wild-type podocin tagged with FLAG at its amino terminus was stained without permeabilization using 0.1% Triton X, suggesting that the amino terminus of podocin was located very close to the plasma membranes within the cells. ×400. *Lower panels* R138Q tagged with FLAG at its amino terminus could not be stained without permeabilization using 0.1% Triton X, suggesting that it remained in the intracellular organelle at a site remote from the plasma membrane. ×400. **b, c** OK cells expressing FLAG-tagged R138Q were fixed without treatment by 0.1% Triton X, then stained with anti-FLAG M2 antibody. In contrast to the *lower right panel* (**a**), 100 mM TMAO (**b**) and 2% DMSO (**c**) enabled staining of FLAG–R138Q along the plasma membrane (indicated by the *arrows*). ×630

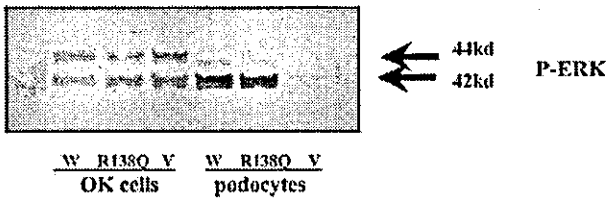

Fig. 6 Induction of ERK2 phosphorylation by transient expression of the wild-type podocin and R138Q podocin. Twenty-four hours after transfection, cells were harvested and proteins were resolved in SDS-PAGE. Western analysis using anti-phosphorylated ERK antibody (Promega) was performed. In a comparison with an empty vector transfection, the expression of the wild-type or R138Q podocins increased the ERK2 (42 kDa) phosphorylation in podocytes. This increase was not evident in the OK cells. Expression of podocins in these samples were shown in Fig. 1

found that the amino terminally FLAG-tagged podocin was immunostained without cell permeabilization with Triton X-100 (Fig. 5a *middle panels*), suggesting that the amino terminus of podocin could be closely located to the plasma membrane within cells. In a previous study, a podocin-related protein called stomatin was found to form a hairpin structure with both of its termini within cells (Salzer et al. 1993; Huang et al. 1995). Though no such structure could be confirmed in our experiment, we did show that the amino terminus of podocin had closer proximity to the plasma membrane than to the carboxy terminus, since immunohistochemistry with myc antibody required permeabilization (Fig. 5a *upper panel*). In contrast to the plasma membrane localization of the wild-type podocin, we clearly showed that the R138Q mutant was retained intracellularly (Fig. 5a *lower panel*). As found with mutant CFTR in cystic fibrosis (Welsh and Smith 1993; Sato et al. 1996) and mutant AQP2 water channels in nephrogenic diabetes insipidus (Tamarappoo and Verkman 1998; Tamarappoo et al. 1999), mistrafficking of these proteins may result from defective folding

or assembly in the ER so that they become recognized by the protein quality control and a substrate for the ER-associated degradation (Yokota et al. 2000; Bückig et al. 2002; Fassio and Sitia 2002; Roth et al. 2002; Schmitz et al. 2002). This could also be true for the R138Q mutation in podocin, given that the close colocalization of R138Q with calnexin confirmed the ER retention of this mutant. In studies using cell culture models, chemical chaperones have been shown to correct protein processing defects associated with several mutations of membrane proteins such as CFTR, and AQP2. In CFTR, exposure of cells to 0.5–1.0 M glycerol resulted in biochemical and functional correction of the deltaF508 CFTR trafficking defect (Sato et al. 1996). Several mechanisms to explain this phenomenon have been proposed. For example, glycerol and related chemical chaperones have been shown to stabilize proteins in vitro and reduce protein aggregation in response to thermal stress (Gekko and Timasheff 1981). Alternatively, glycerol might inhibit the rate of protein synthesis and processing, thereby allowing newly synthesized protein to fold properly (Brown et al. 1996). In this study, two types of chemical promoted the translocation of the R138Q mutant from the ER to the plasma membrane. The colocalization of the cell surface biotin and immunohistochemistry of amino terminally FLAG-tagged R138Q podocin without Triton X-100 treatment (Fig. 5) confirmed the presence of the R138Q mutant in the plasma membrane of the chemical chaperone-treated cells. This clearly suggested that a patient carrying the R138Q mutation might benefit from treatment with these chemicals. However, given the in vivo correction of the R138Q mutant, we know that 1 M glycerol cannot be attained in mammals. As suggested by Tamarappoo and Verkman (1998) in the case of AQP2 mutant, the fish osmolyte TMAO can be maintained at concentrations of 50–75 mM in mice with minimal toxicity. DMSO is already in clinical use for the treatment of amyloidosis in human. Accordingly, these chemical chaperones might provide a clinically useful tool for correcting the podocin protein-folding defect in SRNS patients. Further studies will be necessary to determine if the R138Q released from the ER to the plasma membrane is functionally intact. In the case of AQP2, most of the released missense mutants were found to be functionally intact (Tamarappoo et al. 1999). If podocin does indeed function as a scaffolding protein, the most important factor for podocin to function normally would be to stay at its proper cellular location. In this context, the fact that the intracellular localization of the R138Q was correctable was a good start for this type of strategy. Moreover, the ability to induce ERK2 phosphorylation remained intact even in the mislocalized R138Q, hence the function of R138Q might also remain intact. Further analysis of the ability of R138Q to bind to nephrin may be necessary. In addition, upon the completion of such studies, the administration of these chemicals to transgenic mice carrying this missense mutant will be the only way to obtain a definitive answer.

In summary, our investigation of the molecular pathogenesis of R138Q in the SRNS implicated the mislocalization of the podocin protein in the ER. This ER retention was correctable by chemical chaperones, suggesting possible utility of these agents for the treatment of SRNS patients.

Acknowledgements This study was supported in part by Grants-in-aid from the Ministry of Education, Culture, Sports, Science and Technology of Japan.

References

Boute N, Gribouval O, Roselli S, Benessy F, Lee H, Fuchshuber A, Dahan K, Gubler MC, Niaudet P, Antignac C (2000) NPHS2, encoding the glomerular protein podocin, is mutated in autosomal recessive steroid-resistant nephrotic syndrome. Nat Genet 24:349–354

Brown CR, Hong-Brown LQ, Biwersi J, Verkman AS, Welch WJ (1996) Chemical chaperones correct the mutant phenotype of the delta F508 cystic fibrosis transmembrane conductance regulator protein. Cell Stress Chaperones 1:117–125

Bückig A, Tikkanen R, Herzog V, Schmitz A (2002) Cytosolic and nuclear aggregation of the amyloid precursor peptide following its expression in the endoplasmic reticulum. Histochem Cell Biol 118:353–360

Caridi G, Bertelli R, Carrea A, Di Duca M, Catarsi P, Artero M, Carraro M, Zennaro C, Candiano G, Musante L, Seri M, Ginevri F, Perfumo F, Ghiggeri GM (2001) Prevalence, genetics, and clinical features of patients carrying podocin mutations in steroid-resistant nonfamilial focal segmental glomerulosclerosis. J Am Soc Nephrol 12:2742–2746

Denning GM, Anderson MP, Amara JF, Marshall J, Smith AE, Welsh MJ (1992) Processing of mutant cystic fibrosis transmembrane conductance regulator is temperature-sensitive. Nature 358:761–764

Fassio A, Sitia R (2002) Formation, isomerization and reduction of disulphide bonds during protein quality control in the endoplasmic reticulum. Histochem Cell Biol 117:151–157

Frishberg Y, Rinat C, Megged O, Shapira E, Feinstein S, Raas-Rothschild A (2002) Mutations in NPHS2 encoding podocin are a prevalent cause of steroid-resistant nephrotic syndrome among Israeli–Arab children. J Am Soc Nephrol 13:400–405

Gekko K, Timasheff SN (1981) Mechanism of protein stabilization by glycerol: preferential hydration in glycerol–water mixtures. Biochemistry 20:4667–4676

Hirano K, Roth J, Zuber C, Ziak M (2002) Expression of a mutant ER-retained polytope membrane protein in rat hepatocytes results in Mallory body formation. Histochem Cell Biol 117:45–53

Huang M, Gu G, Ferguson EL, Chalfie M (1995) A stomatin-like protein necessary for mechanosensation in *C. elegans*. Nature 378:292–295

Huber TB, Kottgen M, Schilling B, Walz G, Benzing T (2001) Interaction with podocin facilitates nephrin signaling. J Biol Chem 276:41543–41546

Karle SM, Uetz B, Ronner V, Glaeser L, Hildebrandt F, Fuchshuber A (2002) Novel mutations in NPHS2 detected in both familial and sporadic steroid-resistant nephrotic syndrome. J Am Soc Nephrol 13:388–393

Roth J, Zuber C, Guhl B, Fan J-Y, Ziak M (2002) The importance of trimming reactions on asparagine-linked oligosaccharides for protein quality control. Histochem Cell Biol 117:159–169

Saleem MA, Ni L, Witherden I, Tryggvason K, Ruotsalainen V, Mundel P, Mathieson PW (2002) Co-localization of nephrin, podocin, and the actin cytoskeleton: evidence for a role in podocyte foot process formation. Am J Pathol 161:1459–1466

Salzer U, Ahorn H, Prohaska R (1993) Identification of the phosphorylation site on human erythrocyte band 7 integral membrane protein: implications for a monotopic protein structure. Biochim Biophys Acta 1151:149–152

Sato S, Ward CL, Krouse ME, Wine JJ, Kopito RR (1996) Glycerol reverses the misfolding phenotype of the most common cystic fibrosis mutation. J Biol Chem 271:635–638

Schmitz A, Tikkanen R, Kirfel G, Herzog V (2002) The biological role of the Alzheimer amyloid precursor protein in epithelial cells. Histochem Cell Biol 117:171–180

Schwarz K, Simons M, Reiser J, Saleem MA, Faul C, Kriz W, Shaw AS, Holzman LB, Mundel P (2001) Podocin, a raft-associated component of the glomerular slit diaphragm, interacts with CD2AP and nephrin. J Clin Invest 108:1621–1629

Tamarappoo BK, Verkman AS (1998) Defective aquaporin-2 trafficking in nephrogenic diabetes insipidus and correction by chemical chaperones. J Clin Invest 101:2257–2267

Tamarappoo BK, Yang B, Verkman AS (1999) Misfolding of mutant aquaporin-2 water channels in nephrogenic diabetes insipidus. J Biol Chem 274:34825–34831

Tsukaguchi H, Sudhakar A, Le TC, Nguyen T, Yao J, Schwimmer JA, Schachter AD, Poch E, Abreu PF, Appel GB, Pereira AB, Kalluri R, Pollak MR (2002) NPHS2 mutations in late-onset focal segmental glomerulosclerosis: R229Q is a common disease-associated allele. J Clin Invest 110:1659–1666

Tsutsui T, Yumura W, Nitta K, Nihei H (1997) A stable transfected line of human glomerular epithelial cells. In Vitro Cell Dev Biol 33:489–491

Welsh MJ, Smith AE (1993) Molecular mechanisms of CFTR chloride channel dysfunction in cystic fibrosis. Cell 73:1251–1254

Winn MP (2002) Not all in the family: mutations of podocin in sporadic steroid-resistant nephrotic syndrome. J Am Soc Nephrol 13:577–579

Yokota S, Kamijo K, Oda T (2000) Aggregate formation and degradation of overexpressed wild-type and mutant urate oxidase proteins. Quality control of organelle destined proteins by the endoplasmic reticulum. Histochem Cell Biol 114:433–446

Histochem Cell Biol (2003) 119:485–493
DOI 10.1007/s00418-003-0535-2

ORIGINAL PAPER

Atsushi Hayama · Tatemitsu Rai · Sei Sasaki · Shinichi Uchida

Molecular mechanisms of Bartter syndrome caused by mutations in the BSND gene

Accepted: 6 May 2003 / Published online: 22 May 2003

Abstract Barttin, a gene product of BSND, was identified as a fourth gene responsible for Bartter syndrome. The co-expression of barttin with CLC-K chloride channels has been demonstrated to dramatically induce the expression of CLC-K current. However, it remains unknown how barttin interacts with CLC-K channels in mammalian cells and how the mutations of barttin lead to Bartter syndrome. In an attempt to clarify the effect of barttin expression on CLC-K2 cellular localization, we examined the expression of the CLC-K2 chloride channel and barttin, solely and in combination, in transient and stable expression systems in mammalian cells. In addition, we generated several stable cell lines expressing mutant barttins to clarify the consequence of the previously reported barttin mutations in Bartter syndrome. In immunocytochemistry, CLC-K2 was retained in the Golgi in the absence of barttin expression, but delivered to the plasma membrane when barttin was present. Barttin was coprecipitated with CLC-K2, suggesting a protein–protein interaction. Disease-causing mutant barttins, especially R8L, were retained intracellularly, but their binding ability to CLC-K2 was preserved. This led to a retention of CLC-K2 in intracellular organelles with barttin, and a loss of plasma membrane localization. The stability of the CLC-K2 protein was also markedly increased by coexpression with barttin. These results clarified that barttin determined cellular localization of CLC-K2 by protein–protein interaction. Thus, the mislocalization of CLC-K2 was identified as the molecular pathogenesis of Bartter syndrome by mutant barttins.

Keywords CLC chloride channel · Immunocytochemistry · Protein–protein interaction · Cellular localization

A. Hayama · T. Rai · S. Sasaki · S. Uchida (✉)
Department of Nephrology, Graduate School, School of Medicine, Tokyo Medical and Dental University,
1-5-45 Yushima Bunkyo, 113-8519 Tokyo, Japan
e-mail: suchida.kid@tmd.ac.jp
Tel.: +81-3-58035214, Fax: +81-3-58035215

Introduction

The renal salt loss in Bartter syndrome results from impaired transepithelial sodium chloride transport in the thick ascending limb of Henle's loop and more distal nephron segments (Simon and Lifton 1996). Recently, a positional cloning strategy identified mutations of a new gene (BSND) in a BSND, a variant Bartter syndrome characterized by sensorineural deafness (SND) and renal failure in addition to renal salt loss (Birkenhager et al. 2001). Subsequently, two findings by Esteves et al. (2001) confirmed the function of barttin, a gene product of BSND, as a β-subunit of CLC-K channels. Specifically, they found that barttin was colocalized with CLC-K1 and -K2 chloride channels in mouse kidney, and that the coexpression of barttin induced the human CLC-K current (Estevez et al. 2001). Waldegger (Waldegger et al. 2002) and Esteves presented partial evidence that the barttin-induced CLC-K current was attained by an increase of the cell surface expression of the CLC-Ks, but their experiments were performed only in *Xenopus* oocytes. No studies to date have demonstrated the exact mechanism of the protein interaction of CLC-Ks and barttin, or the cellular localization of these proteins in mammalian cells.

In this study, we examined the expression of CLC-K2 in mammalian cell lines with barttin in order to determine how barttin controls the intracellular localization of CLC-K2. We also investigated the consequence of disease-causing barttin mutations in terms of CLC-K2 intracellular localization. Our results revealed the mechanism by which barttin mutations induce Bartter syndrome. In addition to clarifying the intracellular localizations, we clearly demonstrated a new feature of CLC-K2 protein, i.e., the protein stability with or without barttin expression.

Materials and methods

Construction of CLC-K2 and barttin expression plasmids

Rat CLC-K2 cDNA (Adachi et al. 1994) was cloned into pHM6 expression vector (Roche Diagnostics, Indianapolis, USA) to obtain HA-tagged CLC-K2 at its amino terminus. A CLC-K2 mutant lacking a carboxy terminal cytoplasmic portion was made by inserting a stop codon at K539. A CLC-K2 mutant lacking the first 45 amino acids was generated by PCR. Whole barttin cDNA was obtained by RT-PCR using human kidney mRNA as a template. Primers used were 5′-CCGAATTCGTGTGCAGGCCAGGGACT and 5′-CCGGATCCGCCTTGGGTGTCAGGCTCAAAACC. The amplified cDNA was cut with EcoRI and BamHI at both ends and cloned into EcoRI- and BamHI-cut pCDNA3 myc, His(-)A vector (Invitrogen, Carlsbad, Calif., USA). Point mutations were introduced using a Quick Change site-directed mutagenesis kit (Strategene, La Jolla, Calif., USA). All the sequences of these plasmids were verified by sequencing.

Cell culture and transfection

To isolate the stable transformant, MDCK, COS7, and HeLa cells seeded at approximately 50% confluence in a 3.5-mm plastic were transfected with 2 μg pCDNA3-barttin-myc-His plasmids using Lipofectamine 2000 (Invitrogen). One day after the transfection, the cells were subcultured into five 10-cm dishes in medium containing 2 mg/ml G418 (Invitrogen). About 30 clones were isolated in each construct, and barttin expression was assessed by western analysis using anti-myc antibody (9E10; Santa Cruz Biotechnology, Santa Cruz, Calif, USA). Transient expression of HA-CLC-K2 and barttins were performed in COS7 cells using Fugene6 reagent (Roche Diagnostics) according to the manufacturer's recommendation. Immunocytochemistry was performed 24 h after transfection. Each cell line was maintained in DMEM with 10% fetal bovine serum and 2 mg/ml G418.

Immunocytochemistry

Immunocytochemistry was performed on transfected cells grown on type I collagen-coated coverslips. Briefly, the cells were fixed with 2% paraformaldehyde at 37°C for 30 min and blocked in 1% BSA/PBS at room temperature for 30 min. Next, rat anti-HA antibody (Roche Diagnostics) at 1:200 dilution was added together with mouse monoclonal (9E10) or rabbit polyclonal anti-myc antibody (Santa Cruz Biotechnology) at 1:100 dilution and incubated at room temperature for 1 h. After three 10-min washing steps with blocking buffer, the cells were incubated for 1 h in blocking buffer containing Alexa dye-conjugated species-specific anti-IgG antibodies (Molecular Probes, Eugene, Ore., USA). Subsequently, the sections were washed three times with the blocking buffer, mounted in Quickmount medium (Daido, Japan), and were analyzed by confocal laser scanning microscopy (LMS-5; Zeiss) to determine the subcellular localization of the different proteins. Antibodies to GM130 and calnexin were purchased from BD Bioscience (San Jose, Calif., USA) and Santa Cruz Biotechnology, respectively.

Coimmunoprecipitation

COS7 cells transfected with expression plasmids were lysed in a buffer (150 mM NaCl, 50 mM TRIS, 1% NP40, pH 7.4) for 30 min on ice, then centrifuged for 15 min at 3,000 *g*. The supernatant was rotated at 4°C for 2 h with anti-HA antibody-conjugated beads (Roche Diagnostics). Some of the supernatant was preserved for western blotting. After five washes with a lysis buffer, proteins bound to beads were dissolved in 10 μl 2×Laemmli sample buffer and subjected to SDS-PAGE.

Immunoblotting

Protein denaturation, SDS-PAGE, and blotting were performed as described previously (Uchida et al. 1995). The obtained blots were incubated with 1:200 anti-HA antibody (Roche Diagnostics) or 1:200 anti-myc antibody (9E10) in TBST buffer (20 mM TRIS, 140 mM NaCl, 0.05% Tween 20) with 5% non-fat dried milk. A 1:5,000 dilution of alkaline phosphatase-conjugated anti-rat or -mouse IgG antibody (Promega, Madison, Wis., USA) was used as a secondary antibody, and the signal was detected by western blue (Promega).

CLC-K2 protein stability assay

Adenovirus vector carrying HA-CLC-K2 cDNA was made by an Adenovirus Expression Vector kit (Takara, Japan). Twenty-four hours after infection of the adenovirus vector, the medium was replaced with a methionine- and cysteine-free DMEM containing 10% dialyzed serum. The cells were then incubated for 1 h, and Redivue PRO-MIX (370 MBq/ml) (Amersham Bioscience, Piscataway, N.J., USA) was added (12.5 μl/ml medium). After 1 h of cell labeling, a cell sample at time point 0 was harvested. The medium was then replaced with usual DMEM, and the remaining cells were harvested at each subsequent time point. After lysing the harvested cells in a lysis buffer, labeled CLC-K2 protein was immunoprecipitated using anti-HA antibody-conjugated beads, resolved in SDS-PAGE, and visualized by autoradiography.

Results

Cellular localization of wild-type and mutant barttins in MDCK cells

The protein expressions in MDCK cells were screened by western blotting with anti-myc antibody to isolate stable cell lines expressing wild-type and mutant barttins. At least three cell lines were isolated in each construct, and the consistency of the intracellular localization was confirmed. Figures 1 and 2 show the immunocytochemistry of wild-type and mutant barttins in MDCK cells. As previously reported in vivo, the wild-type barttin was localized in the plasma membrane. However, a significant amount of wild-type barttin protein was also observed intracellularly, probably due to overexpression within the cells. In contrast, the screening for the Y98A mutant resulted in intense staining in the plasma membrane with no intracellular staining observed. This implied that the PY-like motif encompassing Y98 in the barttin protein actually functioned as a motif regulating its own stability in plasma membrane. Such a function would help explain why Y98A induced CLC-K current more than the wild-type in earlier experiments (Estevez et al. 2001).

Figure 2 also shows the intracellular localizations of the disease-causing mutants, R8L and G10S. In contrast to the staining of the wild-type and Y98A, R8L (Birkenhager et al. 2001) was stained intracellularly. Costaining with calnexin, an endoplasmic reticulum (ER) marker, suggested that the R8L mutant was retained in the ER. Another missense mutant, G10S (Birkenhager et al. 2001), was also expressed in MDCK cells, and steps were taken to determine its intracellular localization. Though the G10S staining was also intracellular, there

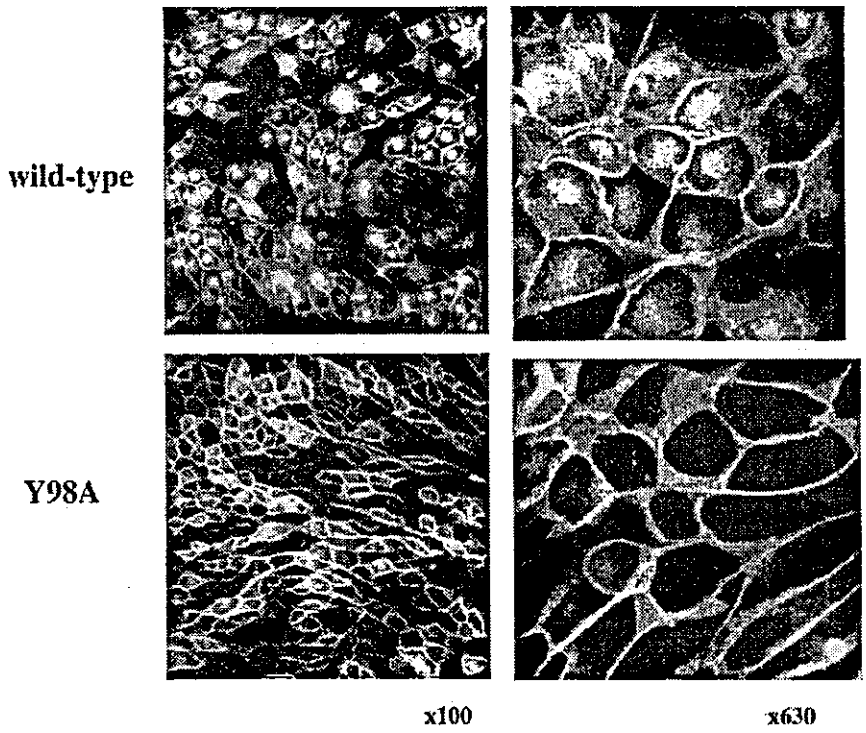

Fig. 1 Immunocytochemistry of wild-type barttin and Y98A mutant stably expressed in MDCK cells. *Left panels* ×100; *right panels* ×630. Myc-tagged barttins were detected with anti-myc antibody (9E10) and Alexa 488-conjugated anti-mouse IgG antibody

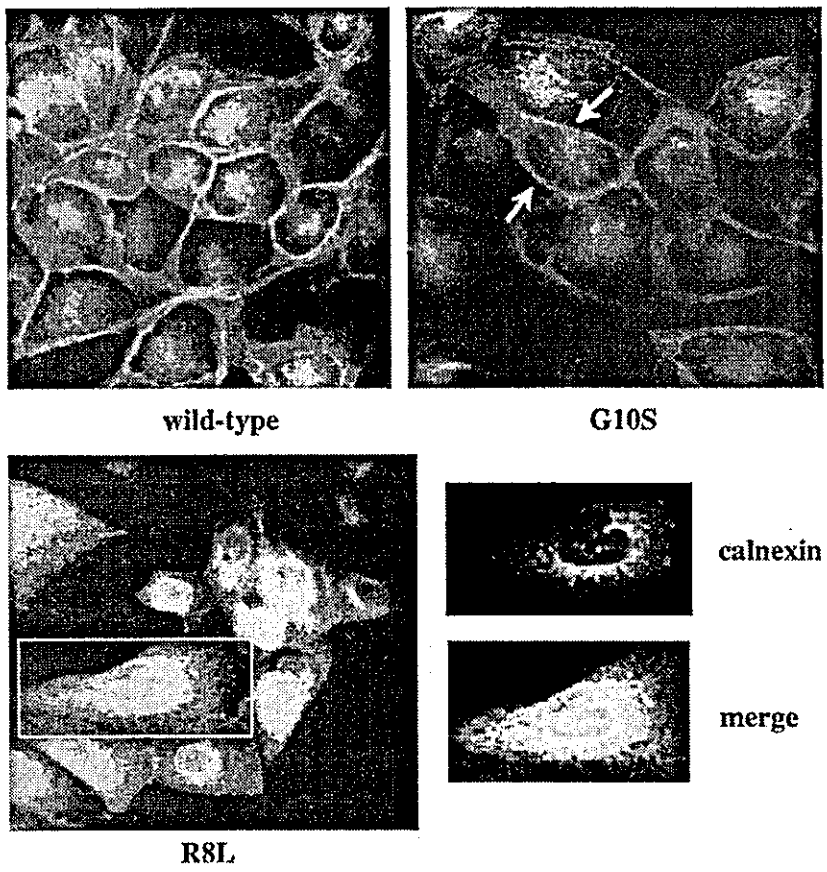

Fig. 2 Immunocytochemistry of disease-causing mutants, R8L and G10S, stably expressed in MDCK cells. Myc-tagged barttins were detected with anti-myc antibody (9E10) and Alexa 488-conjugated anti-mouse IgG antibody. ×630. *Arrows* indicate the plasma membrane staining of G10S. R8L was costained with calnexin

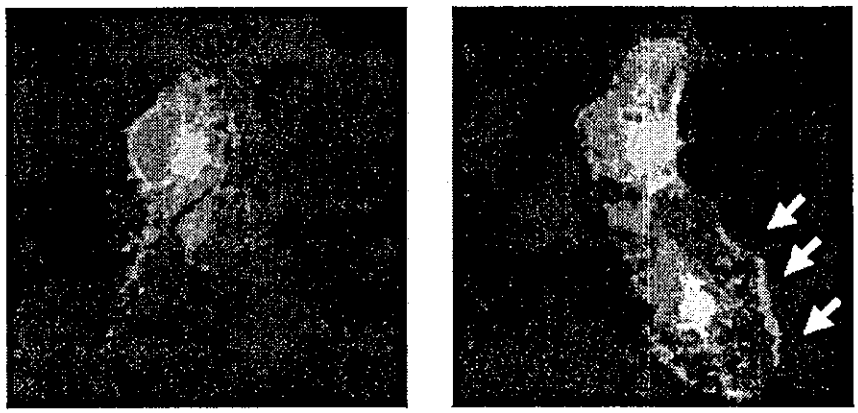

Fig. 3 Immunocytochemistry of CLC-K2 in COS7 cells with and without barttin expression. HA-tagged CLC-K2 was transiently expressed in wild-type COS7 cells and cells stably expressing wild-type barttin. CLC-K2 immunocytochemistry was performed with rat anti-HA antibody (Roche Diagnostics) and Alexa 488-conjugated anti-rat IgG antibody. *Arrows* indicate the plasma membrane localization of CLC-K2. ×630

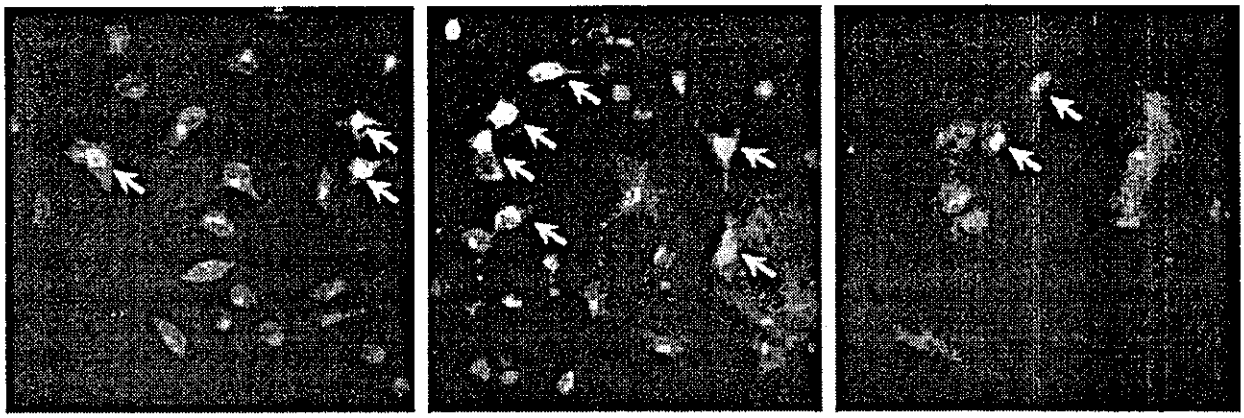

Fig. 4 Intracellular localization of CLC-K2 without barttin coexpression. COS7 cells transiently expressing CLC-K2 were costained with anti-GM130 (Golgi marker) and calnexin (ER marker). CLC-K2 is shown in green, and GM130 (*center*) and calnexin (*right*) are shown in red. ×40. CLC-K2 staining in green was merged to yellow with GM130 staining in red. *Arrows* indicate CLC-K2 immunostaining

was some plasma membrane staining as well, revealing a localization different from that of R8L. Accordingly, G10S showed an intermediate phenotype between the wild-type and R8L, in terms of the plasma membrane localization within our expression system. This may be related to the finding by Estevas (Estevez et al. 2001), who showed that G10S was capable of increasing the CLC-K current in the same manner as the wild-type.

Intracellular localization of CLC-K2 with or without barttin expression

To investigate the effect of barttin expression on the cellular localization of CLC-K2, HA-tagged CLC-K2 was transiently expressed in COS7 cells stably expressing wild-type barttin. An attempt to express CLC-K2 protein in the MDCK cells stably expressing barttins proved unsatisfactory, even with the use of an adenovirus vector expression system. As shown in Fig. 3, CLC-K2 was recruited to the plasma membrane in the presence of barttin expression, whereas the staining remained intracellular in the absence of barttin expression. To determine the CLC-K2 localization without barttin expression, CLC-K2 was costained with GM-130 and calnexin, a Golgi marker and ER marker, respectively. As shown in Fig. 4, CLC-K2 staining (green) was colocalized with GM130, suggesting that CLC-K2 was retained in the Golgi in the absence of barttin coexpression.

Intracellular localization of CLC-K2 with mutant barttins

To reveal the pathogenesis of Bartter syndrome by barttin mutations, we determined the intracellular localization of CLC-K2 when coexpressed with mutant barttins. In cells

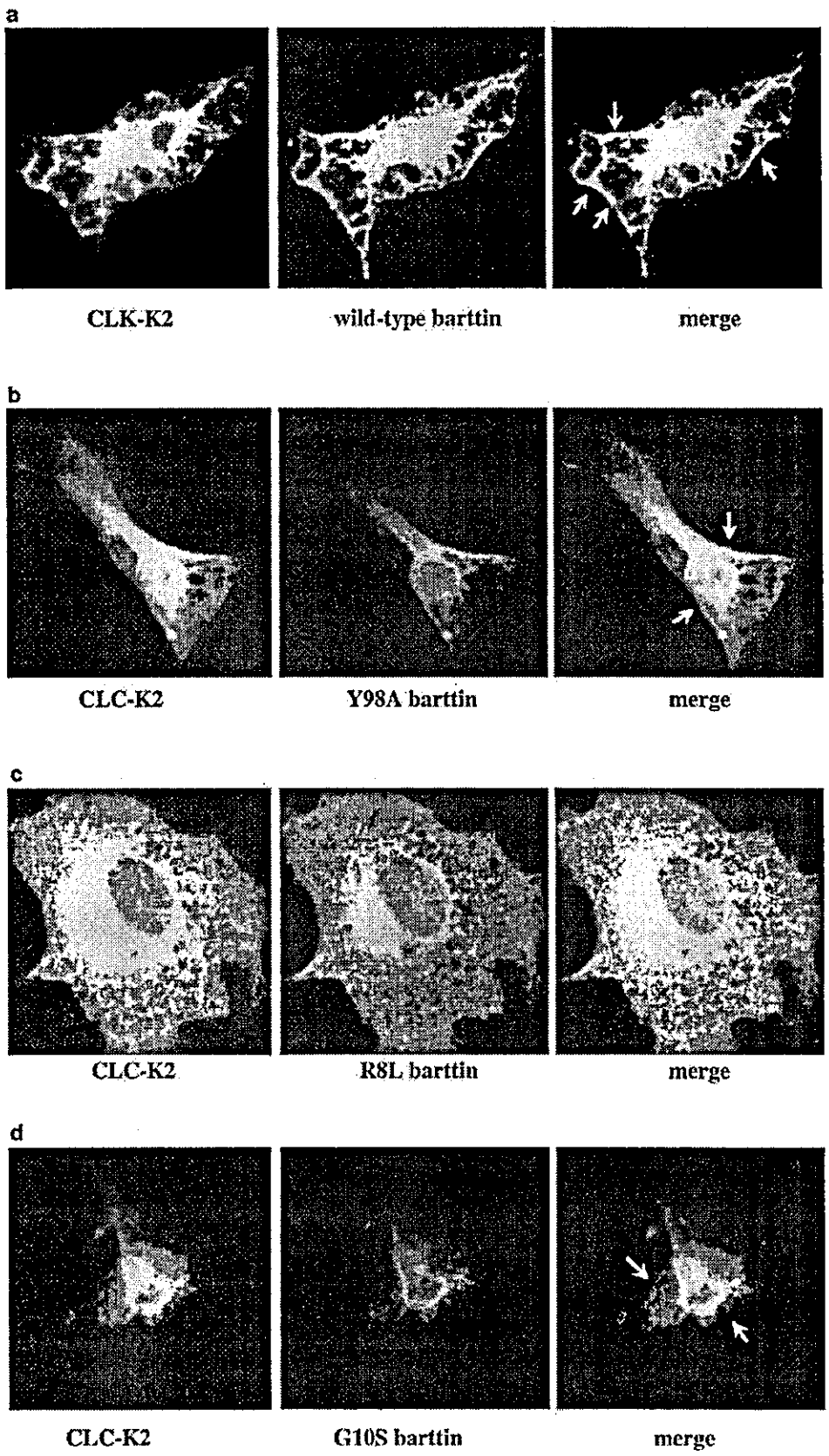

Fig. 5a–d Colocalization of CLC-K2 and wild-type and mutant barttins. a Colocalization of CLC-K2 (green) and wild-type barttin (red). *Arrows* indicate colocalization. ×630. b Colocalization of CLC-K2 (green) and Y98A barttin (red). *Arrows* indicate colocalization. ×630. c Colocalization of CLC-K2 (green) and R8L barttin (red). ×630. d Colocalization of CLC-K2 (green) and G10S barttin (red). ×630. *Arrows* indicate the surface expression of CLC-K2 and barttin

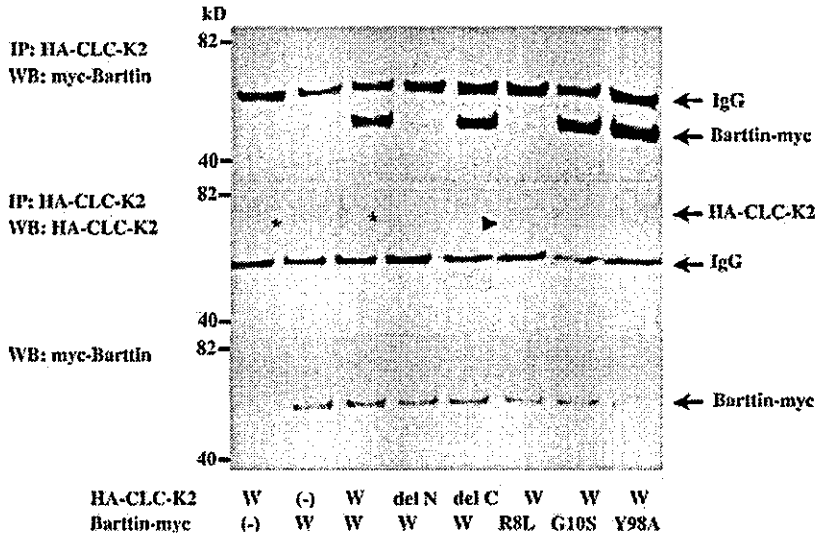

Fig. 6 Coimmunoprecipitation of CLC-K2 and barttins. Plasmids transfected were indicated in each lane below the lower panel. *W* indicates wild-type. *del N* and *del C* indicate amino and carboxy terminal deletion of CLC-K2. An *arrowhead* indicates immunoprecipitated CLC-K2 coexpressed with R8L. *Asterisks* in *lanes 1* and *3* indicate immunoprecipitated CLC-K2

expressing wild-type and Y98A barttins, CLC-K2 was colocalized with barttin in the plasma membrane (Fig. 5a, b). In contrast, CLC-K2 was almost completely colocalized with R8L intracellularly in the cells expressing R8L barttin (Fig. 5c). Thus, the recruitment of CLC-K2 to plasma membrane was impaired. CLC-K2 was also almost completely colocalized with G10S, another missense mutant that leads to disease. However, G10S was also detectable in the plasma membrane as shown in Fig. 1, and CLC-K2 could be found there with it.

Coimmunoprecipitation of CLC-K2 and barttin

A coimmunoprecipitation study was performed to investigate whether the HA-CLC-K2 and barttin-myc are physically interacted (Fig. 6). Initially, HA-CLC-K2 and barttin-myc were transiently expressed in COS7 cells. After immunoprecipitating samples with anti-HA antibody, two western blots of the immunoprecipitants were performed: one with anti-myc antibody to investigate their interaction (*upper panel*) and one with anti-HA antibody to confirm the expression of CLC-K2 (*middle panel*). In addition, western blot of cell lysates was performed with anti-myc antibody to confirm the barttin expression (*lower panel*). As shown in the *lower panel*, wild-type and mutant barttins were almost equally expressed in COS7 cells. The *third* and *last lanes* in the *upper panel* show that wild-type and Y98A barttins were coimmunoprecipitated with wild-type CLC-K2, respectively. Although the CLC-K2 expression was weak in the lane for R8L (*sixth lane* in the *middle panel*), R8L (*sixth lane*) and G10S (*seventh lane*) were also coimmunoprecipitated with wild-type CLC-K2. This result was consistent with the intracellular colocalization of CLC-K2 and mutant barttins shown in Fig. 5c, d. The crystal structure of bacterial CLC chloride channels was recently resolved (Dutzler et al. 2002). The channels form a homodimer, and most of the protein is embedded in a lipid bilayer. Accordingly, it was speculated that only the amino and carboxy termini could bind to its own accessory proteins in cytoplasm. To determine whether these parts of CLC-K2 were involved in the binding to barttin, CLC-K2 mutants lacking either the amino or carboxy terminal cytoplasmic portion were coexpressed with wild-type barttin. Although the CLC-K2 mutant lacking amino terminal portion (*fourth lane*) was expressed poorly in the cells, barttin could also be immunoprecipitated (*upper panel*), ruling out the involvement of these two cytoplasmic regions of CLC-K2 in the binding to barttin. It may be that barttin binds to CLC-K not at a defined small domain, but on the relatively broad surface of the CLC-K protein.

CLC-K2 protein stability

It was also interesting to find out in our coimmunoprecipitation experiment that CLC-K2 expression (Fig. 6 *first* and *third lanes* in the *middle panel*) was consistently weaker in the absence of barttin expression than it was in its presence (Fig. 6 *asterisks*). This difference in CLC-K2 expression suggested that barttin could also be involved in CLC-K2 protein stability. To investigate this possibility, we measured CLC-K2 protein stability in the presence or absence of barttin expression. HA-CLC-K2 was expressed using an adenovirus vector (Takara) in the wild-type and barttin-expressing HeLa cells. As shown in Fig. 7, the half-life of CLC-K2 protein with barttin expression was much longer than that without it. The CLC-K2 protein rapidly degraded without barttin expression, exhibiting a very short half-life of less than 1 h.

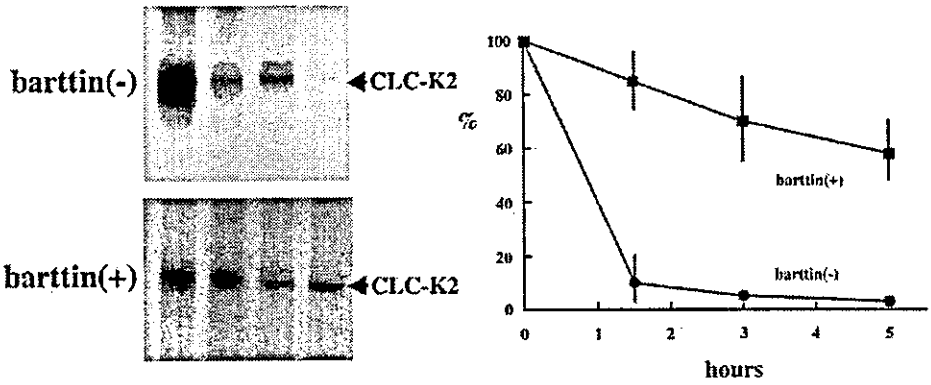

Fig. 7 CLC-K2 protein stability with and without barttin expression. Wild-type HeLa cells and cells expressing barttin were infected with adenovirus vector containing HA-CLC-K2 cDNA. Twenty-four hours after infection, cells were labeled with ^{35}S-methionine and cysteine for 1 h and chased. HA-CLC-K2 was immunoprecipitated using anti-HA antibody-conjugated agarose beads, resolved in SDS-PAGE, and visualized by autoradiography. The intensity of the bands was measured using a BAS2000 system (Fuji, Japan) and expressed as a percentage of time 0 (n=3, mean ± SD)

Discussion

Several studies, including our own (Adachi et al. 1994; Akizuki et al. 2001; Kieferle et al. 1994; Kobayashi et al. 2001a, b, 2002; Matsumura et al. 1999; Uchida et al. 1993, 1995; Waldegger and Jentsch 2000), have established the physiological roles of CLC-K chloride channels in vivo. On the other hand, there have been almost no studies on the cellular localizations and their regulation of these proteins in cell culture systems. The identification of barttin as a β-subunit of CLC-K chloride channels (Estevez et al. 2001) sheds light on these unexplored aspects of CLC-K channels. In this study, we determined the intracellular localizations of the CLC-K2 protein with and without wild-type and disease-causing mutants of barttin. These results clarified the interaction of CLC-K and barttin within mammalian cells and revealed the molecular mechanisms by which barttin mutations lead to Bartter syndrome.

By generating stable cell lines expressing wild-type and mutant barttins, we could clearly identify their intracellular localizations (Figs. 1, 2). To begin with, it was surprising to find an almost total absence of intracellular staining of the Y98A mutant, since the overexpression system often produces the abundant intracellular staining, as observed in the wild-type. Some light was shed on the function of this PY-like motif (PQPPY) by previous physiological evidence (Estevez et al. 2001) showing an increase in the coexpressed CLC-K current by the mutation of PQPPY to PQPPA. Using immunocytochemistry in this study, we confirmed that the PY-like motif is indeed involved in the degradation of barttin in the plasma membrane. As suggested by Schwake et al. (2001) in their work with CLC-5, some ubiquitin-protein ligases could bind to this PY-like motif and take part in the degradation of the target proteins in the plasma membrane. Through a mechanism reminiscent of the epithelial sodium channel (ENaC) in Liddle syndrome (Schild et al. 1996), mutation at this PY-like motif could increase transepithelial chloride conductance in the thick ascending limb of Henle's loop, thereby increasing sodium chloride reabsorption and producing salt-sensitive hypertension. Further screening for mutations in the BSND gene may be necessary in hypertensive patients.

This is the first demonstration of the intracellular localization of disease-causing barttin mutants. As shown in Fig. 2, the R8L mutant was apparently localized in the ER. In previously observations of membrane proteins such as CFTR (Welsh and Smith 1993), vasopressin V2R receptor, and AQP2 water channel (Tamarappoo et al. 1999), some missense mutations influenced the process of protein folding and the mutants were subjected to degradation within the ER. R8L may also be involved in such quality control mechanisms of the ER. The localization of G10S, another disease-causing mutant, was not completely intracellular, as substantial G10S staining could be observed in the plasma membrane of stable MDCK cell lines. In experiments using *Xenopus* oocytes expressing G10S and CLC-K, Estevas (Estevez et al. 2001) found that G10S induced the CLC-K current. Thus, all studies to date, including our own, have failed to elucidate the pathogenesis of G10S. It may be that overexpression forces the G10S retained in the ER to leak out to the plasma membrane. G10S might be retained mainly in the ER on the level of physiological expression as well.

To clarify the effect of barttin mutation on the cellular localization of CLC-K2, we unsuccessfully attempted to express CLC-K2 in these MDCK cell lines. Even with the use of an adenovirus vector carrying the CLC-K2 insert, western analysis and immunocytochemistry both failed to detect the CLC-K2 protein. The same problem has impeded studies on the CLC-K protein in heterologous expression systems for many years, and the exact mechanisms remain unknown. The problem may stem

from the rapid degradation of the CLC-K protein within cells, as shown in Fig. 7. Accordingly, numerous trials have been made to find a cell line suitable for the expression of CLC-K2 protein, and the COS7 cells were found to be best in terms of the immunocytochemical study of CLC-K2. As clearly shown in Fig. 3, CLC-K2 was present in Golgi when expressed alone. When coexpressed with wild-type and mutant barttins (Figs. 4, 5), however, CLC-K2 appeared to be taken by barttins to the sites where barttins resided within cells. These results strongly suggested that wild-type and even mutant barttins could bind CLC-K2.

Therefore, we performed a coimmunoprecipitation experiment to confirm the protein–protein interactions of CLC-K and barttins. Waldegger et al. (2002) attempted a similar study in *Xenopus* oocytes, but the immunoprecipitated band of CLC-K protein did not match the estimated molecular weight of CLC-K, and thus their results were not convincing. As shown in Fig. 6, wild-type CLC-K2 bound to the mutant barttins as well as the wild-type. This quite nicely explained why even the mutant barttins could control the cellular localization of CLC-K2, as observed earlier in our immunocytochemical investigation. Thus, our study showed that, rather than affecting the interactions with CLC-K2, the barttin mutations affected their own cellular localization.

Our immunoprecipitation experiment also turned up evidence of a potential mislocalization of R8L. The apparent molecular weight of CLC-K2 differed between a sample coexpressed with R8L (Fig. 6 *sixth lane*) and a sample coexpressed wild-type barttins (Fig. 6 *third lane*). We show in Fig. 4 that CLC-K2 is mainly present in Golgi without barttin expression. This is consistent with a previous finding by Jentsch's group (Kieferle et al. 1994), i.e., CLC-K channel expressed in oocyte without barttin underwent glycosylation. Thus, the difference of molecular weight might have been based on the presence or absence of glycosylation of CLC-K2, since CLC-K2 might have been primarily retained in the ER and prevented from reaching the Golgi when coexpressed with R8L.

Another interesting finding in this immunoprecipitation experiment was the difficulty in expressing and detecting CLC-K2 protein. As shown in the *middle panel* of Fig. 6, western blot determined the level of CLC-K protein in immunoprecipitated materials, but not in cell lysates. As shown by the *asterisks* in Fig. 6, the expression of CLC-K2 protein expressed alone was always weaker than that of CLC-K2 expressed with wild-type barttin. This prompted us to measure stability of the CLC-K2 protein. Measurements were taken in several cell lines to obtain more consistent results, and the most consistent measurements proved to be in HeLa cells. After generating a stable cell line expressing wild-type barttin in HeLa cells, we induced the expression of HA-CLC-K2 using adenovirus vector in order to maximize the expression of CLC-K2. As shown in Fig. 7, the turnover of CLC-K2 protein was very rapid in the absence of barttin coexpression. This might explain why we encountered such difficulty in our previous trial to detect CLC-K2 protein in the heterologous expression system before ascertaining the presence of barttin. Given that the level of CLC-K2 was always lower in coexpression with R8L than with the wild-type, we know that the mechanisms of this stabilization cannot be explained solely by the binding of barttin to CLC-K2. If the barttin binding masks some important residues in CLC-K2 involved in CLC-K2 degradation, R8L might also increase CLC-K2 stability. This suggested that both the binding and the localization in plasma membrane were important for stabilizing CLC-K2 protein.

In summary, we demonstrated the intracellular localization of CLC-K2 and wild-type and mutant barttins in mammalian cells as well as the protein–protein interactions of these proteins. Our findings clearly illustrated how the barttin mutations lead to Bartter syndrome.

Acknowledgements This study was supported in part by grants-in-aid from the Ministry of Education, Culture, Sports, Science, and Technology of Japan, and the Salt Science Research Foundation.

References

Adachi S, Uchida S, Ito H, Hata M, Hiroe M, Marumo F, Sasaki S (1994) Two isoforms of a chloride channel predominantly expressed in thick ascending limb of Henle's loop and collecting ducts of rat kidney. J Biol Chem 269:17677–17683

Akizuki N, Uchida S, Sasaki S, Marumo F (2001) Impaired solute accumulation in inner medulla of Clcnk1–/– mice kidney. Am J Physiol Renal Physiol 280:F79–F87

Birkenhager R, Otto E, Schurmann MJ, Vollmer M, Ruf EM, Maier-Lutz I, Beekmann F, Fekete A, Omran H, Feldmann D, Milford DV, Jeck N, Konrad M, Landau D, Knoers NV, Antignac C, Sudbrak R, Kispert A, Hildebrandt F (2001) Mutation of BSND causes Bartter syndrome with sensorineural deafness and kidney failure. Nat Genet 29:310–314

Dutzler R, Campbell EB, Cadene M, Chait BT, MacKinnon R (2002) X-ray structure of a ClC chloride channel at 3.0 A reveals the molecular basis of anion selectivity. Nature 415:287–294

Estevez R, Boettger T, Stein V, Birkenhager R, Otto E, Hildebrandt F, Jentsch TJ (2001) Barttin is a Cl^- channel beta-subunit crucial for renal Cl^- reabsorption and inner ear K^+ secretion. Nature 414:558–561

Kieferle S, Fong P, Bens M, Vandewalle A, Jentsch TJ (1994) Two highly homologous members of the ClC chloride channel family in both rat and human kidney. Proc Natl Acad Sci U S A 91:6943–6947

Kobayashi K, Uchida S, Mizutani S, Sasaki S, Marumo F (2001a) Developmental expression of CLC-K1 in the postnatal rat kidney. Histochem Cell Biol 116:49–56

Kobayashi K, Uchida S, Mizutani S, Sasaki S, Marumo F (2001b) Intrarenal and cellular localization of CLC-K2 protein in the mouse kidney. J Am Soc Nephrol 12:1327–1334

Kobayashi K, Uchida S, Okamura HO, Marumo F, Sasaki S (2002) Human CLC-KB gene promoter drives the EGFP expression in the specific distal nephron segments and inner ear. J Am Soc Nephrol 13:1992–1998

Matsumura Y, Uchida S, Kondo Y, Miyazaki H, Ko SB, Hayama A, Morimoto T, Liu W, Arisawa M, Sasaki S, Marumo F (1999) Overt nephrogenic diabetes insipidus in mice lacking the CLC-K1 chloride channel. Nat Genet 21:95–98

Schild L, Lu Y, Gautschi I, Schneeberger E, Lifton RP, Rossier BC (1996) Identification of a PY motif in the epithelial Na channel

subunits as a target sequence for mutations causing channel activation found in Liddle syndrome. EMBO J 15:2381–2387
Schwake M, Friedrich T, Jentsch TJ (2001) An internalization signal in ClC-5, an endosomal Cl-channel mutated in Dent's disease. J Biol Chem 276:12049–12054
Simon DB, Lifton RP (1996) The molecular basis of inherited hypokalemic alkalosis: Bartter's and Gitelman's syndromes. Am J Physiol 271:F961–F966
Tamarappoo BK, Yang B, Verkman AS (1999) Misfolding of mutant aquaporin-2 water channels in nephrogenic diabetes insipidus. J Biol Chem 274:34825–34831
Uchida S, Sasaki S, Furukawa T, Hiraoka M, Imai T, Hirata Y, Marumo F (1993) Molecular cloning of a chloride channel that is regulated by dehydration and expressed predominantly in kidney medulla. J Biol Chem 268:3821–3824
Uchida S, Sasaki S, Nitta K, Uchida K, Horita S, Nihei H, Marumo F (1995) Localization and functional characterization of rat kidney-specific chloride channel, ClC-K1. J Clin Invest 95:104–113
Waldegger S, Jentsch TJ (2000) Functional and structural analysis of ClC-K chloride channels involved in renal disease. J Biol Chem 275:24527–24533
Waldegger S, Jeck N, Barth P, Peters M, Vitzthum H, Wolf K, Kurtz A, Konrad M, Seyberth HW (2002) Barttin increases surface expression and changes current properties of ClC-K channels. Pflugers Arch 444:411–418
Welsh MJ, Smith AE (1993) Molecular mechanisms of CFTR chloride channel dysfunction in cystic fibrosis. Cell 73:1251–1254